Blue light enhanced Heck arylation at room temperature applied to allenes

(Article begins on next page)

30 June 2024

ARTICLE

Blue Light Enhanced Heck Arylation at Room Temperature Applied to Allenes

Polyssena Renzi,[a] Emanuele Azzi,[a] Enrico Bessone,[a] Giovanni Ghigo,*[a] Stefano Parisotto,[a] Francesco Pellegrino,[a] and Annamaria Deagostino *[a]

An unprecedented visible light enhanced room temperature Heck reaction between aryl halides and allenyl tosyl amines is here reported. The simple catalytic system (Pd(OAc)$_2$/PPh$_3$) is exploited to afford arylated vinyl pyrrolidines and piperidines in good to excellent yields. A broad scope with high tolerance towards functional groups is presented. Electronic effects play an important role in the efficiency of this process. Mechanistic studies, both experimental and computational, indicates no evidence for a radical mechanism and a pivotal role of the light in promoting the carbo-palladation step.

Introduction

Among small drugs and pharmaceutically relevant molecules, alkaloids have a leading role as witnessed by the percentage of FDA approvals and availability on the market which raised from 59% to more than 75% over the last 6 years.[1-4] Among them, those related to pyrrolidine and piperidine are the most common five- and six-membered aliphatic *N*-heterocycles.[5-8] Some valuable examples are reported in Figure 1. Consequently, the development of efficient and general methodologies for their preparation is of paramount importance.[9]

natural alkaloids

Hygrine
from coca leaves

Anisomycin
from Streptomyces griseolus

(+)-Allosedamine
from indian tobacco

active pharmaceutical ingredients

Remoprixide
antipsychotic

Methylphenidate
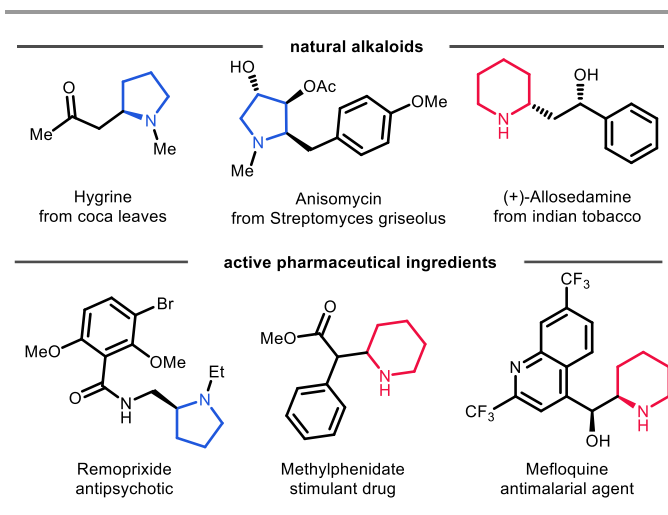stimulant drug

Mefloquine
antimalarial agent

Fig. 1 Selected examples of pyrrolidines and piperidines present in pharmaceuticals and natural alkaloids.

*a. Department of Chemistry, University of Torino
Via Pietro Giuria, 7 – 10125 Torino (Italy).*
E-mail: annamaria.deagostino@unito.it; giovanni.ghigo@unito.it
Electronic Supplementary Information (ESI) available: [details of any supplementary information available should be included here]. See DOI: 10.1039/x0xx00000x

Differently from their aromatic counterparts, there are limited strategies to access substituted saturated *N*-heterocycles with ease and efficiency.[10] They fall into two main categories: the cyclization of suitable precursors and the modification of readily available pyrrolidines and piperidines. The latter approach can be accomplished by α-lithiation, C(sp^3)–H activation, mainly exploiting radical mechanisms and directing groups, or redox-neutral C–H functionalisation.[9, 11] Concerning cyclisations, many efforts have recently been devoted to the development of greener strategies (including solvent- or metal-free, one-pot, microwave assisted and in aqueous media).[12] Nevertheless, transition metal catalysed reactions still dominate this scenario. Grubbs and Fu were the first to apply the ring-closing metathesis (RCM) to the synthesis of simple *N*-containing five-, six-, and seven-membered monocyclic systems.[13] Several methodologies relying on Rh, Au or Fe have also been reported.[10] Anyway, a pivotal role is played by Pd. Named reactions such as Ullmann−Goldberg, Buchwald−Hartwig[14] and aza−Heck[15-17] are frequently applied to form new C−N bonds affording saturated heterocycles.

Recently, the interest towards these transformations has pushed researchers to look for alternative conditions in order to lower the reaction temperature while keeping the efficiency high in term of both yield and selectivity. Examples of room temperature Heck reactions were reported by Zhang[18] and Larrosa[19] exploiting respectively phenylsulfonium salts as coupling partners, or silver salts in combination with 1,1,1,3,3,3-hexafluoropropan-2-ol (HFIP) as the solvent. Silver(I) salts were also used to accomplish the decarboxylative Heck coupling of carboxylic acids and electron-deficient substrates.[20] A step forward towards room temperature cross-coupling reactions was made by studying the application of light irradiation. In 2010, the group of Köhler observed, for the first time, the acceleration of a Heck reaction under UV-visible light using both homogeneous or heterogeneous Pd(II) pre-catalysts.[21] Few years later, Gevorgyan disclosed an original visible light-induced room temperature Heck reaction between functionalised alkyl

halides and styrenes.[22] The same coupling was not possible *via* a traditional thermal reaction, thus indicating the crucial role of the light in the photoexcitation of the Pd(0) catalyst and opening an orthogonal reactivity not possible under classical conditions. That was the starting point for the employment of transition metal complexes, especially those containing Pd, as unconventional photocatalysts.[23-25] With such approach, remarkable papers dealing with the coupling of alky halides and the decarboxylative coupling of redox-active esters were published by the research groups of Gevorgyan,[22, 26-28] Fu,[29, 30] Königs,[31] Glorius[32, 33] and Rueping.[34] Moreover, visible-light Pd(0) catalysis was used for the radical cross-coupling of $C(sp^3)$–H bonds with non-activated bromides,[35] in an intermolecular Nasaka−Heck reaction *via* the photoactivation of N−O bonds[36] and for the synthesis of *C*-glycoside styrenes.[37] In the above-mentioned transformations, a radical mechanism was generally hypothesised, involving a barrierless oxidative addition of the substrate (*e.g.* alkyl halides) to a photoexcited Pd(0) complex.

Since 2003, when we reported our first synthetic effort in the use of 1-alkoxy-1,3-dienes in Pd(0) catalysis,[38] our group has continued working on the Heck reaction applied to allylic substrates deriving form alkoxyallenes, alkoxydienes[39-41] and vinyl epoxides[42, 43] affording, *via* cascade processes, highly functionalized unsaturated molecules.[44] Thus, from our experience on π-allyl complexes, we settled on merging UV-visible light with palladium catalysis to explore allenes as reagents in novel reactivity pathways. Under conventional conditions, allenes have been extensively employed in inter- and intra-molecular Heck reactions producing numerous complex cyclic skeletons.[23, 24, 45-50] Despite allenes unique reactivity and great synthetic potential, their application in light-mediated reactions is currently limited.[51-54] To our knowledge, no examples of their use in visible-light promoted Pd(0) processes have been reported so far. In this framework, we present a blue light enhanced room temperature Heck reaction between aryl halides and allenyl tosyl amines, producing valuable branched vinyl pyrrolidines and piperidines *via* a domino carbo-amination. Mechanistic investigations were realized in order to understand the role of the light in the catalytic cycle.

Results and discussion

To prove the feasibility of a room temperature Pd(0) Heck reaction on allenes promoted by visible light, we chose substrate *N*-tosylhexa-4,5-dien-1-ylamine **1a** as a model (see ESI for its synthesis). After screening several Pd(0) precursors, phosphines, solvents and bases, we found out that the coupling between allene **1a** and bromobenzene **2a** could indeed be achieved at room temperature to afford vinyl pyrrolidine **3a**. Optimal reaction conditions involved 5 mol% of Pd(OAc)$_2$, 10 mol% of PPh$_3$, 1.2 eq. of K$_2$CO$_3$ in anhydrous DMF under irradiation from a 40W Kessil blue LED lamp. Under such conditions, pyrrolidine **3a** was produced in 92% yield from 0.1 mmol of **1a** and in 70% yield on 0.2 mmol scale (Table 1 entry 1). According to the efficiency of the catalytic system, 3-methyl-

N-tosyl-2-(*N*-tosylpyrrolidynil)-epta-2,3-dienamine **4a**, a dimer of **1a**, could be found as by-product. No conversion of **1a** was observed when the reaction was carried out at room temperature in the absence of the irradiation or of the base (Table 1, entries 2 and 4). The lack of either PPh$_3$ or halide **2a** caused the complete degradation of allene **1a** (Table 1, entries 3 and 5), while no conversion was achieved excluding simultaneously the phosphine and bromobenzene **2a** (Table 1 entry 6).

To further confirm the essential role played by the light, the same transformation was attempted under thermal conditions (see ESI for the complete study). At 60°C without light, product **3a** was isolated in a reduced yield of 45% (Table 1, entry 7). Merging light irradiation with heating, pyrrolidine **3a** was obtained in only 40% yield with an increase in dimer amount to 14% (Table 1, entry 8). These results indicated no synergic effect between light and thermal energy. More than that, purple light was not as efficient as the blue one, indeed **3a** was produced in 43% yield, together with 10% of the dimer side-product **4a** (Table 1, entry 9).
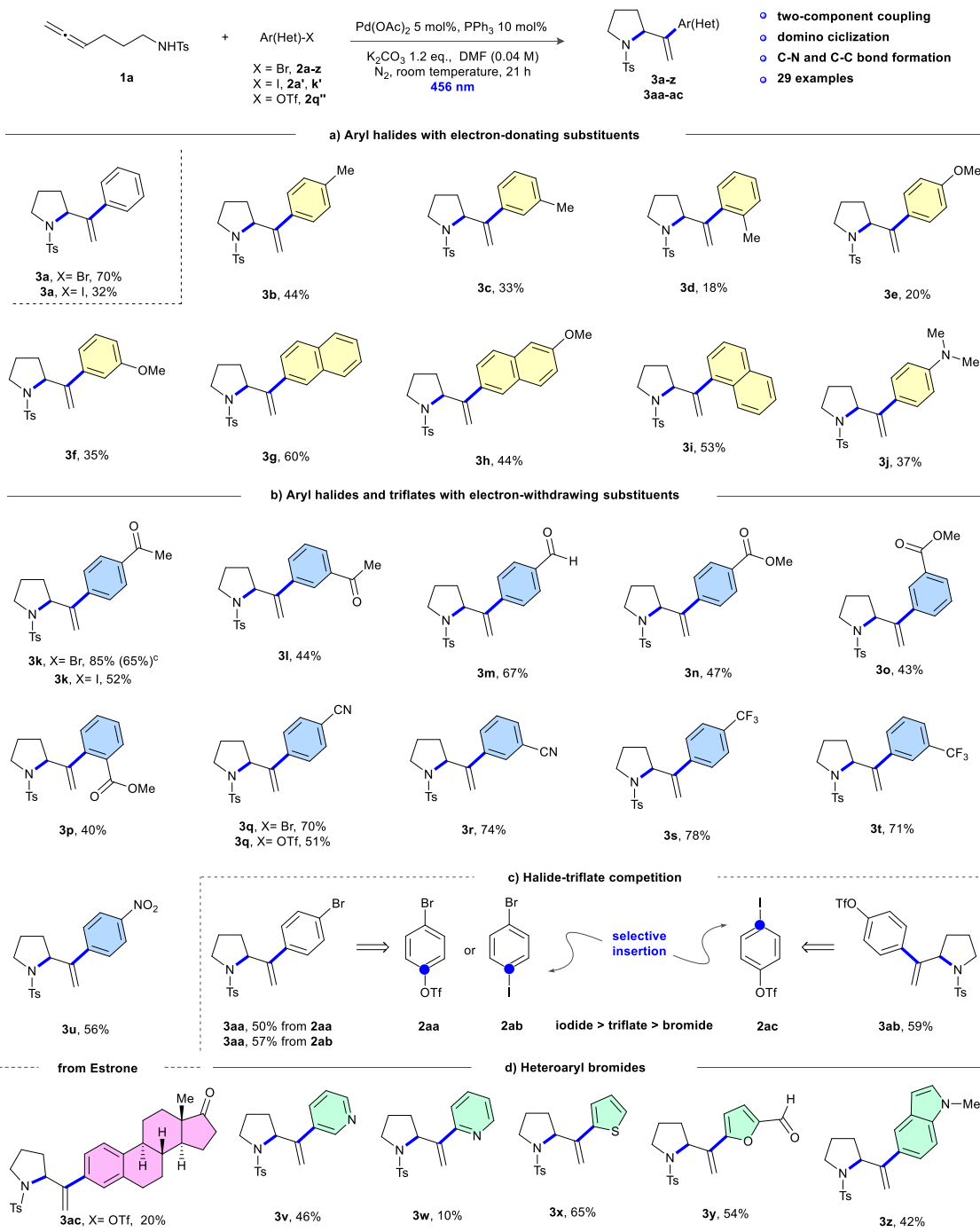
Table 2: Optimisation of reaction conditions.
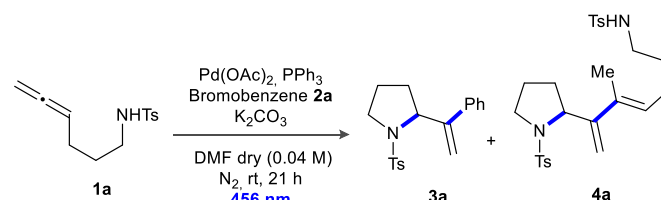
Entry	Deviation	3a Yield [%][b]	4a Yield [%][b]
1	none[a]	70[a] / 92[c]	4[a] / 0[c]
2[c]	no irradiation	0	0
3[c]	no PPh$_3$	degradation	
4[c]	no K$_2$CO$_3$	0	0
5	no **2a**	degradation	
6	no **2a**, no PPh$_3$	0	0
7	60°C, no irradiation	45	4
8	60°C, irradiation	40	14
9	purple LEDs	43	10
10	AcONa	0	66
11	Pd(PPh$_3$)$_4$	0	0
12	Xantphos	29	0

[a] Optimal conditions: allenyl tosyl amine **1a** (0.2 mmol), Pd(OAc)$_2$ (5 mol%), PPh$_3$ (10 mol%), K$_2$CO$_3$ (0.24 mmol, 1.2 eq.), PhBr **2a** (0.3 mmol, 1.5 eq.) in anhydrous DMF (0.04 M), 40W Kessil blue LED lamp (456 nm), 21 h, room temperature. [b] Determined on the isolated product. [c] Reaction carried out on 0.1 mmol of allenyl amine **1a**.

Following these findings, reaction conditions were extensively screened in order to assess the role of the base, the phosphine, the solvent and the pre-catalyst (see ESI for exhaustive Tables). The outcome was highly dependent on the base and on the palladium source with the readily available Pd(OAc)$_2$ being the most effective one among those tested. Notably, when we evaluated the performance of catalytic systems commonly employed in reactions triggered by a single electron transfer event,[31, 32, 55] we had unsatisfying results (Table 1, entry 11 and 12). Pd(PPh$_3$)$_4$ did not promote any

ARTICLE

Table 2: Scope of the reaction for the synthesis of substituted *N*-tosyl-1-aryl-1-vinylpyrrolidines **3a-z**, **3aa-ac**[a,b]

Reaction scheme: **1a** + Ar(Het)-X (X = Br, **2a-z**; X = I, **2a', k'**; X = OTf, **2q''**) → Pd(OAc)₂ 5 mol%, PPh₃ 10 mol%, K₂CO₃ 1.2 eq., DMF (0.04 M), N₂, room temperature, 21 h, 456 nm → **3a-z**, **3aa-ac**

- two-component coupling
- domino ciclization
- C-N and C-C bond formation
- 29 examples

a) Aryl halides with electron-donating substituents

3a, X= Br, 70%
3a, X= I, 32%

3b, 44%

3c, 33%

3d, 18%

3e, 20%

3f, 35%

3g, 60%

3h, 44%

3i, 53%

3j, 37%

b) Aryl halides and triflates with electron-withdrawing substituents

3k, X= Br, 85% (65%)[c]
3k, X= I, 52%

3l, 44%

3m, 67%

3n, 47%

3o, 43%

3p, 40%

3q, X= Br, 70%
3q, X= OTf, 51%

3r, 74%

3s, 78%

3t, 71%

c) Halide-triflate competition

3u, 56%

3aa, 50% from **2aa**
3aa, 57% from **2ab**

2aa

2ab

selective insertion

iodide > triflate > bromide

2ac

3ab, 59%

from Estrone

d) Heteroaryl bromides

3ac, X= OTf, 20%

3v, 46%

3w, 10%

3x, 65%

3y, 54%

3z, 42%

[a] Reaction conditions: *N*-tosylhexa-4,5-dien-1-ylamine **1a** (0.2 mmol), Pd(OAc)₂ (5 mol%), PPh₃ (10 mol%), K₂CO₃ (0.24 mmol, 1.2 eq.), aryl (pseudo)halide (0.3 mmol, 1.5 eq.) in anhydrous DMF (0.04 M), 40W Kessil blue LED lamp (456 nm), 21 h, room temperature. [b] Yields determined on the isolated products. [c] Reaction performed on 1 mmol of allene **1a**.

Table 3: Scope of the reaction for the synthesis of substituted *N*-tosyl-1-aryl-1-vinylpiperidines **5a-o**[a,b]
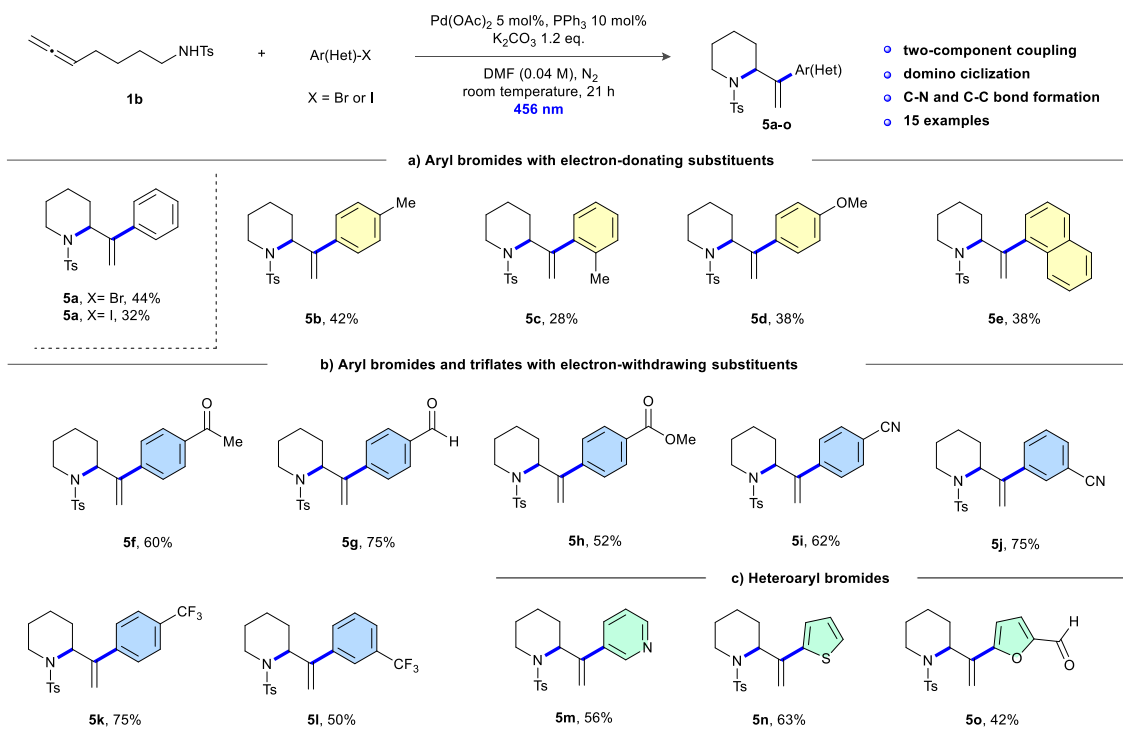
[a] Reaction conditions: *N*-tosylhepta-5,6-dien-1-ylamine **1b** (0.2 mmol), Pd(OAc)$_2$ (5 mol%), PPh$_3$ (10 mol%), K$_2$CO$_3$ (0.24 mmol, 1.2 eq.), aryl halide (0.3 mmol, 1.5 eq.) in anhydrous DMF (0.04 M), 40W Kessil blue LED lamp (456 nm), 21 h, room temperature. [b] Yields determined on the isolated products.

conversion of the starting allene, while Pd(OAc)$_2$/Xantphos delivered pyrrolidine **3a** in only 29% yield. Regarding the base, we observed a complete suppression of the desired carbo-amination in favour of the dimerization when K$_2$CO$_3$ was replaced by the weaker AcONa. That being so, diene **4a** was produced in 66% yield (Table 1, entry 10). An additional screening of reagent amounts and ratios (described in the ESI) confirmed the condition reported in Table 1 entry 1 to be the optimal. Thus, a simple set up composed by commercially available Pd(OAc)$_2$, PPh$_3$ and a mild inorganic base, under irradiation from blue LEDs at room temperature in the presence of bromobenzene **2a**, enabled the efficient Heck reaction with allene **1a** to afford vinyl pyrrolidine **3a**.

With the optimized conditions, we extended the carbo-amination scope to several aryl bromides spanning from electron-rich (Table 2a) to electron-poor (Table 2b) and heteroaryl (Table 2d) substrates. Some examples employing aryl iodides and triflates were also reported. Despite the generality of the reaction, a remarkable influence of the substituents was observed. Electron-donating groups generally hampered the reactivity of the corresponding aryl bromides **2a**-**j** regardless of the substitution pattern. Yields below 50% were observed, with the only exception being product **3g**, which was isolated from 2-bromonaphthalene **2g** in 60% yield. Nevertheless, methyl, methoxy aryl and dimethylamino groups were tolerated. A pronounced steric effect was also noticed. For example, moving from the *para* to the *ortho* isomer of bromotoluene, a further dramatic drop in the reactivity gave product **3d** in only 18% yield. Accordingly, such effect was not observed on *meta*

substituted arenes, and comparable results were obtained with 3-bromotoluene **2c** and 3-bromo-anisole **2f** with products **3c** and **3f** recovered in 33% and 35% yield. On the contrary, from good to excellent results were achieved from electron-poor aryl bromides (see Table 2b, products **3k**-**u**). Yields up to 85% were observed and several functionalised arenes were installed on the vinyl pyrrolidine scaffold. It is worth mentioning the strategic positioning of the acetyl, formyl, carboxymethyl, nitrile and nitro moieties (products **3k**-**r** and **3u**) for their possible exploitation in step-wise syntheses. Looking at the wide diffusion of fluorinated molecules in medicinal chemistry, we were delighted by the successful reaction with 3- and 4-bromobenzotrifluoride, which delivered pyrrolidines **3s**-**t** in very good yields, 78% and 71% respectively.

3-Bromobenzonitrile **2r** was as efficient as the *para* isomer (**3q**, **3r**: 70% and 74%). A slightly diminished yield was observed with 4-bromobenzaldehyde **2m**, with a value of 67% (**3m**). Independently from the position of the ester group, similar results were obtained for methyl bromobenzoates **2n**-**p**, with yield between 40% (**3p**, *ortho*) and 47% (**3n**, *para*). The presence of the ester group in *meta* or *ortho* position with respect to the bromine atom did not significantly influence the performance of the carbo-amination. High tolerance was also demonstrated toward the nitro group, indeed pyrrolidine **3u** was isolated in 56% yield. Heteroaryl bromides could be employed as well, both electron-rich and -poor, with good outcomes, except for 2-bromopyridine **2w**. N-, O- and S-, five and six membered arenes were successfully introduced (Table 2d). Noteworthy, the densely functionalized furane **3y** was isolated in 54% yield.

Moreover, the process was scaled up by a factor of 5 without significant erosion in yield (**3k**, 65% yield on 1 mmol vs 85% on 0.2 mmol, Table 2b). In addition, a reductive desulfonylation of **3a** afforded the free secondary amine (see ESI compound **3a'**). Then, we tested the reactivity of aryl iodides and triflates, which were proven able to incorporate aryl moieties on the vinyl pyrrolidine scaffold too. Nevertheless, under blue light we observed a superior reactivity efficacy associated with aryl bromides. Indeed, pyrrolidine **3a** was produced in a modest 32% from iodobenzene **2a'** (70% from bromobenzene). Electron-poor triflates performed better and benzonitrile **3q** was isolated in 51% yield, but again worse than from the corresponding bromide (70%). Given those results, we run competitions experiments to get a reactivity scale of the (pseudo)halides (Table 2c). 4-Bromo- and 4-iodo triflates **2aa** and **2ac** gave derivatives **3aa** and **3ab** with similar efficiency, but opposite chemoselectivity. While the carbon-iodine bond was cleaved in triflate **2ac**, the latter moiety was replaced on bromide **2aa**. Finally, 1-bromo-4-iodobenzene **2ab** selectively reacted at the iodide terminal, affording bromoarene **3aa** in 57% yield. The observed high chemoselectivity could be further exploited in consecutive metal-catalysed transformation to prepare complex molecules in a controllable manner. Moreover, the successful reaction on aryl triflates, translates in the possible late-stage modification of natural phenols and pharmaceuticals by exploiting the oxygenated reactive site as we demonstrated for the triflate derived from estrone. Product **3ac** was obtained in a 20% yield. Furthermore, we extended the scope to *N*-tosylhepta-5,6-dien-1-ylamine **1b**. Under same conditions, a selection of (hetero)aryl bromides was reacted to access a small library of vinyl piperidines **5a**-**o** (Table 3), showing results consistent with those summarized in Table 2. Again, electron-poor arenes were introduced more efficiently than electron-rich ones. With few exceptions, the carbo-amination was not influenced by the increased dimension of the ring formed and piperidines **5a**-**o** were isolated with yields similar to the corresponding pyrrolidines. Only bromobenzene **2a** and 1-bromonaphthalene **2i** gave modest results. The highest yield of 75% was obtained for 4-bromobenzaldehyde **2m**, 3-bromobenzonitrile **2r** and 4-bromobenzotrifluoride **2s**. Regarding the heteroaryl bromides, the preparation of piperidinyl vinyl pyridine **5m** in 56% yield was remarkable. Indeed, the easiest method for constructing substituted piperidines undoubtedly is the catalytic reduction of pyridines.[56, 57] However, this reaction usually suffers from poor functional group tolerance. The preparation of piperidine **5m** *via* a similar strategy would therefore require a challenging hydrogenation of a substrate containing two pyridyl rings, in addition to a more reactive olefin. In such context, our carbo-amination protocol can easily overcome such chemoselectivity issue. Piperidine **5a** was also prepared from iodobenzene **2a'** in 32% yield, demonstrating again the superior behaviour of bromoarenes. The scope was completed with internal allenes **1c** and **1d**. For such substrates, a longer reaction time was required, however the complete conversion of the starting allenyl amine was observed after 48 hours. Similar yields and electronic effects from the substituent on the aryl bromide

were observed (Table 4). Products **6a**-**d**, **7a**-**d** were isolated as mixture of diastereomers. Besides pyrrolidines **6a** and **7a**, where a 99:1 and 64:36 diasteromeric ratio was respectively measured, all other reactions had selectivity higher than 80:20. A predominance of the *E* isomer was proved by 2D-NOE analysis on both isolated diasteroisomers of **6d** (see ESI).

Table 4: Scope of the reaction in internal allenes **1c**-**d**[a-d]
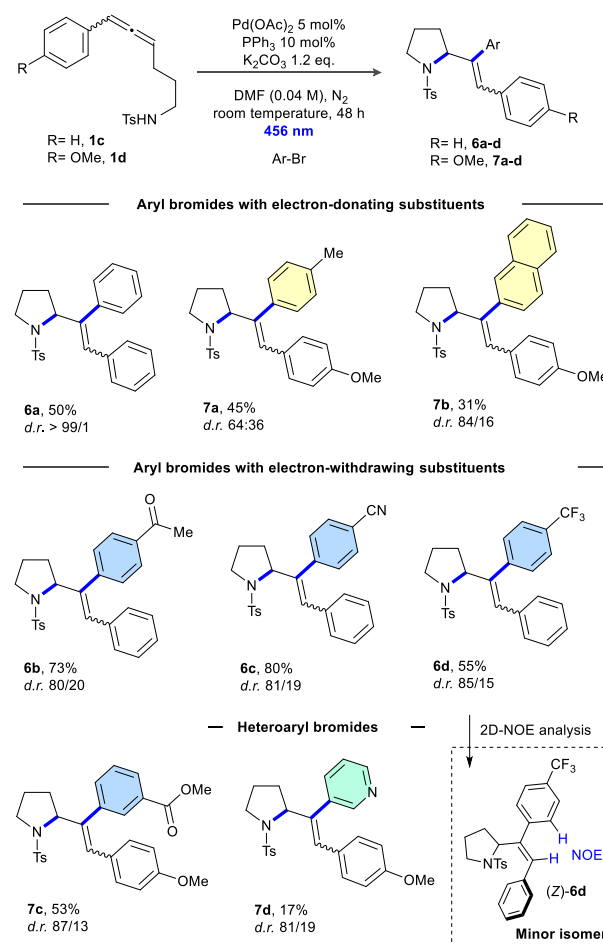
[a] Reaction conditions: allene **1c** or **1d** (0.2 mmol), Pd(OAc)$_2$ (5 mol%), PPh$_3$ (10 mol%), K$_2$CO$_3$ (0.24 mmol, 1.2 eq.), aryl bromide (0.3 mmol, 1.5 eq.) in anhydrous DMF (0.04 M), 40W Kessil blue LED lamp (456 nm), 48 h, room temperature. [b] Yields determined on the isolated products. [c] Diastereomeric ratio calculated on the crude mixture by ^{1}H-NMR. [d] NOESY experiments were employed to determine the configuration of the double bond.

Mechanistic Studies: Experimental and Computational

In order to understand the role of the blue light in this room temperature Heck reaction, we carried out a mechanistic investigation. Inspired by the literature published on similar reactions,[33, 58-60] we performed UV-Vis and fluorescence emission analyses of the catalytic system. As shown in Figure 2a, absorption from a diluted solution of Pd(OAc)$_2$/2PPh$_3$ (8 mM in DMF) was observed in the visible region (black line), with peaks at 415 and 505 nm. After the addition of bromobenzene **2a** a modification of this profile took place.
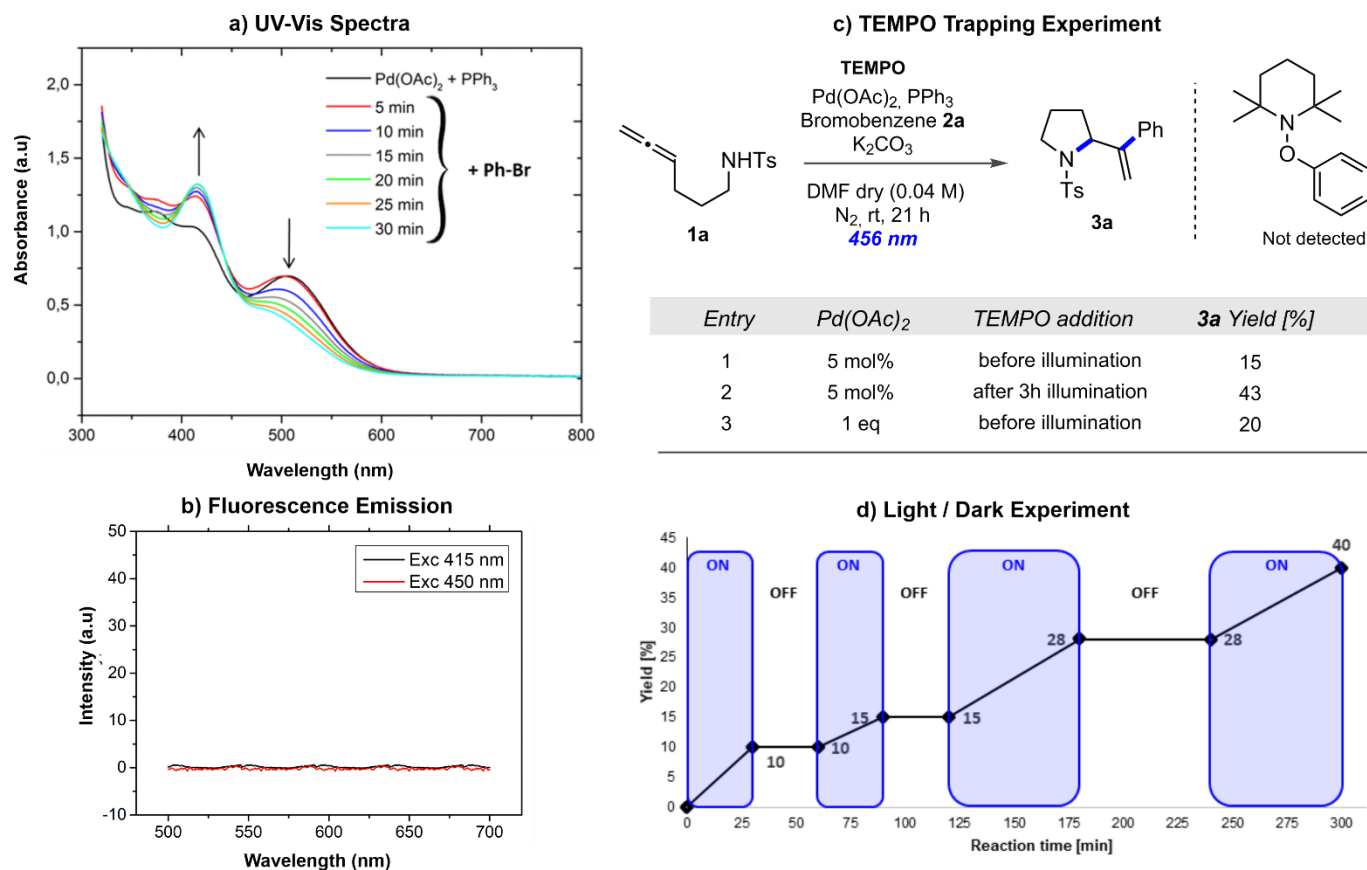
ARTICLE

Fig. 2 [a] UV-Vis spectra of a 8 Mm solution of the catalyst Pd(OAc)$_2$-PPh$_3$ 1:2 (black line) as such and after the addition of bromobenzene **2a** at different intervals of time. [b] Fluorescence emission in the range 500-700 nm upon excitation at 415 nm (black line) and 450 nm (red line). [c] Light/Dark experiment. [d] TEMPO trapping experiment. Details of the experimental conditions for each study are reported in the ESI.

The evolution of the spectra with time showed a slow and progressive decrease of the absorption at 505 nm with a concomitant fast increase of the peak intensity at 415 nm (substantial after just 5 minutes), suggesting the feasibility of the oxidative addition at room temperature (Figure 2a). This change of the system characteristics has been also observed in the electrochemical analysis reported in the ESI.

The results from the UV-Vis study were employed for the fluorescence analysis,[58] but no fluorescence was detected upon excitation at 415 and 450 nm while monitoring the emission in the range 500-700 nm (see Figure 2b). Therefore, we repeated the standard optimized reaction between allene **1a** and bromobenzene **2a** in the presence of TEMPO radical (Figure 2c). The formation of a phenyl radical-TEMPO adduct was not confirmed and only a substantial suppression of the carbo-amination was observed. This is consistent with the ability of *N*-

oxyl radicals to oxidize Pd(0) species,[61, 62] thus interfering with this specific catalytic cycle. Such observations are substantially different from those reported in the literature using Pd(PPh$_3$)$_4$, involving radical intermediates and single electron reduction of the electrophile.[24, 63] Despite these findings, the fundamental role of the light in promoting this Heck reaction was proved by a light-dark experiment (Figure 2d), which clearly showed the evolution of the reaction exclusively under continuous irradiation.

NMR spectroscopy was also exploited to gain mechanistic insights into the process. ^{31}P-NMR monitoring of the catalytic system (Figure 3a) in DMF-*d$_7$* (*vs* H$_3$PO$_4$ 85% as reference) in the absence of blue light showed the formation of different species. The spectra recorded in our study were in accordance with the results published by Amatore *et al.* in DMF-*d$_7$*,[60] and more recently by the group of Fairlamb in THF-*d$_8$*.[64, 65]
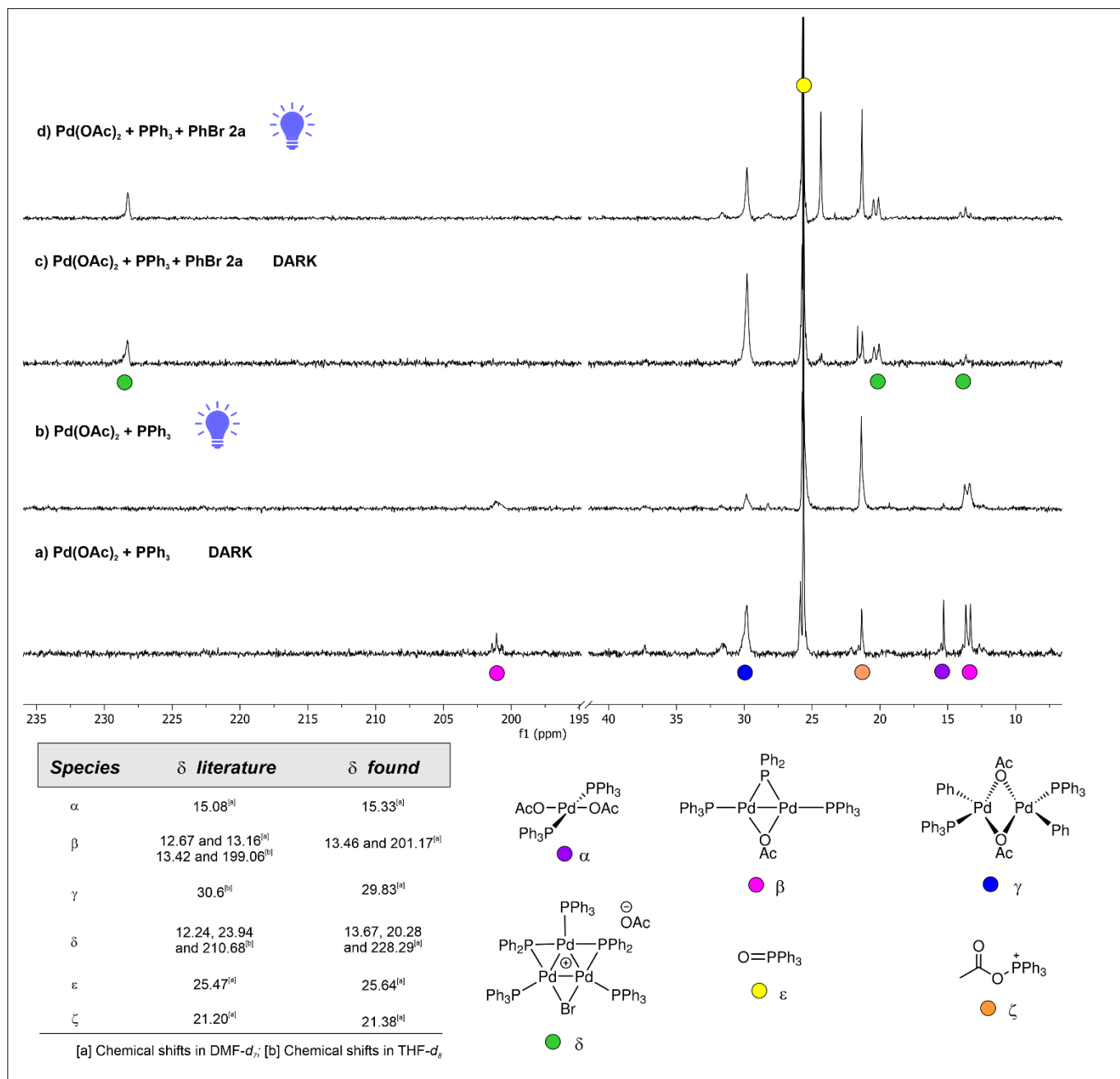
ARTICLE

Fig. 3 ^{31}P-NMR (242 MHz) spectra in DMF-d_7 at room temperature of mixtures of: [a] Pd(OAc)$_2$ with 2 PPh$_3$; [b] Pd(OAc)$_2$ with 2 PPh$_3$ after irradiation for 2 h with 40W Kessil blue LED lamp (456 nm); [c] Pd(OAc)$_2$ with 2 PPh$_3$ and bromobenzene **2a**; [d] Pd(OAc)$_2$ with 2 PPh$_3$ and bromobenzene **2a** after irradiation for 2 h with 40W Kessil blue LED lamp (456 nm). Bottom: the table showed the experimental chemical shifts compared with those reported in the literature[60, 64, 65] for species **α–ζ** which structures are depicted on the right.

The reduction of the $Pd(OAc)_2/2PPh_3$ mixture proceeded via formation of *trans*-[Pd(OAc)$_2$(PPh$_3$)$_2$] α, of the dinuclear [Pd$_2$(μ-PPh$_2$)(μ$_2$-OAc)(PPh$_3$)$_2$] complex β and the dimeric Pd(II) species γ (for chemical shifts see Figure 3 bottom). Those compounds could act as a reservoir of precursors which may be gradually converted to the active Pd(0) catalyst. Moreover, signals at 21.38 and 25.64 ppm were respectively assigned to [(AcO)PPh$_3$]$^+$ ζ and to triphenylphosphine oxide ε, key side products from Pd(II) reduction. In the absence of light, both signals corresponding to low valent Pd catalyst precursors (compounds α and β) disappeared when brombenzene **2a** was added to the catalyst solution (Figure 3c), in analogy to what observed by Amatore with iodobenzene,[60] indicating that the oxidative addition of **2a** was feasible at room temperature as previously proved by UV-Vis measurements. Three novel signals were detected and tentatively assigned to cluster δ or to a similar species. In the same way, we investigated the catalytic system under irradiation. Solutions of Pd(OAc)$_2$/2PPh$_3$ in DMF-d_7 with and without halide **2a** were irradiated for 2 hours at 456 nm. As shown in Figure 3b and 3d, the same active species were present in both irradiated and not irradiated mixtures, except for *trans*-[Pd(OAc)$_2$(PPh$_3$)$_2$] α. As suggested by Köhler, blue light seems to play a role in accelerating the rate of the reduction of Pd(II) precursors by influencing the distribution of metastable intermediates in favour of compound β. Upon addition of **2a**, intermediate β was immediately consumed as observed also in the dark, with the formation of an additional signal at 24.36 ppm which was not observed in the absence of light. Free PPh$_3$ could not be detected in any of our samples.

Even though blue light might accelerate the formation of the active Pd(0) catalyst, the requirement for continuous irradiation demonstrated by the light/dark experiment pointed toward an additional role of the blue light in this specific carbo-amination reaction. Therefore, quantum chemical calculations[66, 67] were performed to study the different pathways involved in the thermal and photochemical reaction.

As shown in the optimization of the reaction conditions, the optimal ratio Pd(II)/PPh$_3$ for the reduction of the pre-catalyst Pd(AcO)$_2$ is 1:2. Despite the precursors detected by ^{31}P-NMR, we assumed that the active catalyst is Pd^0(PPh$_3$), formed according the following net equation:

$$Pd(OAc)_2 + 2 PPh_3 \rightarrow Pd^0(PPh_3) + O=PPh_3 + Ac_2O$$
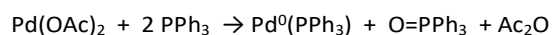
The calculated reaction energy for this process (including explicit DMF molecules that makes Pd^0(PPh$_3$) a stable 18 e- species, (see ESI) is -40.9 kcal mol^{-1} in terms of free energy

Starting from the active Pd(0) catalyst **I**, the first reaction step was assumed to be the oxidative insertion of the aryl bromide **II** yielding intermediate **III** (Figure 4). This process was calculated to be exoergic by 11.0 kcal mol^{-1} and it should easily occur being its barrier (TSA) only 5 kcal mol^{-1} with respect to the complex formed between **I** and **II** (4 kcal mol^{-1} with respect to the reactants). The release of two DMF molecules makes Pd(0) a reactive 14 e- species, able to bound bromobenzene. The low

barrier, although probably underestimated, is coherent with the quite fast change in the UV-Vis spectra of the catalyst mixture after the addition of bromobenzene **2a** (Figure 2a).

Coherently with the experimental observation of a reduction of the yields when larger amount of PPh$_3$ are used, we observed that the oxidative addition to Pd^0(PPh$_3$)$_2$ (also a 14 e- species generated from three equivalents of PPh$_3$) is still exoergic (ΔG = -12.3 kcal mol^{-1}) but sensibly slower. The free energy barrier (with respect to the reactants) is 14.5 kcal mol^{-1} higher (18.3 kcal mol^{-1}, see details in the SI) than that with Pd^0(PPh$_3$).

The transition structures for the oxidative addition optimized here are similar to that found in recent computational papers for the same catalyst and aryl halides.[67, 68]
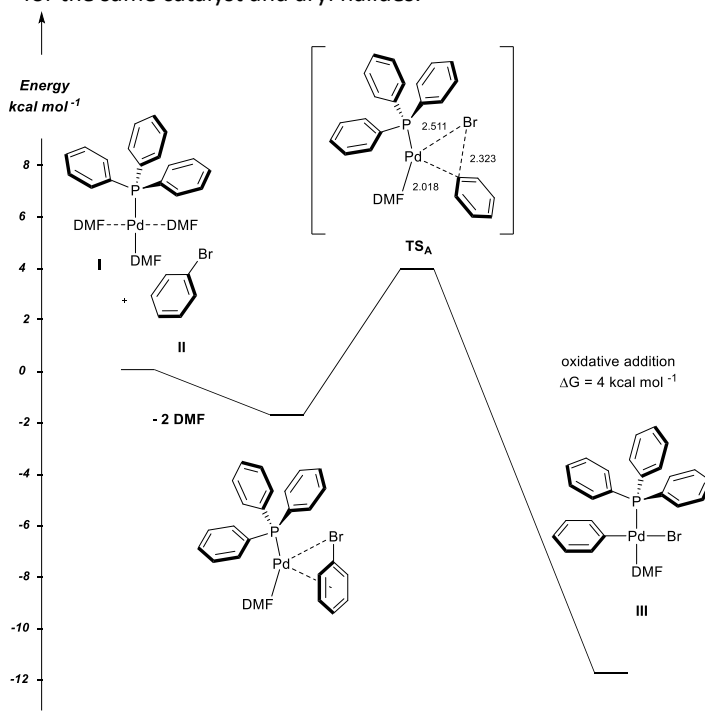

Fig. 4 Energy profiles in kcal mol^{-1} for the oxidative addition of the bromobenzene **II** to the catalyst **I**.

More interesting for the present work is the study of the reaction mechanism in the presence of the allene. Once **III** is thermalized in the environment, it can react with the deprotonated allene **IV$^-$** following different pathways. The favourite one consists in the formation of intermediate **A** after release of a DMF molecule and the capture of anion **IV$^-$** (red profiles in Figure 5). In this case, the palladium atom is complexed to the allene *via* a π interaction with the unsaturated moiety. The irreversible migration of the phenyl group from palladium to the central sp carbon of the allene (**TS$_B$**) yields intermediate **B**. A change in the conformation (conformer **B'**) allows the formation of a new C–N bond which yields intermediate **C** through **TS$_C$**. The final decoordination of the bromide ligand and the capture of three DMF molecules regenerates catalyst **I** delivering the final product **P**.

Alternatively (green profiles, Figure 5), intermediate **A** might bind the anionic nitrogen to palladium yielding intermediate **D**

which, upon release of the bromide, forms intermediate **E**. **TS_D** resulted to be 1.4 kcal mol⁻¹ lower than **TS_B**.

As shown by the blue profile in Figure 5, an alternative pathway, again starting from **III** and **IV⁻**, is also possible. The deprotonated allene can, in fact, bind to palladium through its anionic nitrogen substituting the bromide thus forming intermediate **F**. The latter after the release of a DMF molecule, forms again **E**. Intermediates **A**, **D** and **E** are quite close in free energy (between -5 and -10 kcal mol⁻¹ with respect to **III** + **IV⁻**), and they can be easily formed through **TS_B**, **TS_D** or **F** (only 5 – 8 kcal mol⁻¹ above **III** + **IV⁻**).

Under thermal condition, the evolution of intermediate **E** is not energetically favoured. In fact, the phenyl migration through **TS_G** to yield intermediate **G** costs in free energy 36 kcal mol⁻¹ with respect to **E** and yet almost 30 kcal mol⁻¹ with respect to **III** + **IV⁻**. As we see later, photochemical pathways can overcome this difficulty allowing intermediate **E** to have a key role. Once intermediate **G** is formed, the migration of the nitrogen from palladium to the carbon, through **TS_H**, yields the intermediate **H** that, after the capture of three DMF molecules yields again the final products **I** and **P**.

Alternatively (see ESI), the intermediate **G** can undergo the migration of one hydrogen atom from the carbon to the palladium. This pathway is not competitive.

Intermediate **E**, for which we calculated an optically active electronic transition at 432 nm (in this case with the toluenesulfonyl group), can be excited to the S_1 state located at 64 kcal mol⁻¹ (blue profile, Figure 6). After vibrational relaxation (VR), the singlet excited **¹E*** gives rise to the phenyl migration through **¹TS*_G** with a barrier of only 7.7 kcal mol⁻¹ (compared to 35.9 for the ground state). Finally, intermediate **¹G***, which is located at -46.1 kcal mol⁻¹ with respect to **¹E***, decays to the ground state **G** that can evolve towards the final product.

Alternatively (orange profile, Figure 6), the same process can take place through the triplet states after Inter-System Crossing (ISC) from **¹E*** and VR. First, the intermediate **³E*** is formed, then, through **³TS*_G**, the phenyl migration takes place with an activation energy of 6.6 kcal mol⁻¹. Finally, the intermediate **³G*** decays to its ground state **G** so the reaction can proceed as described in Figure 5.
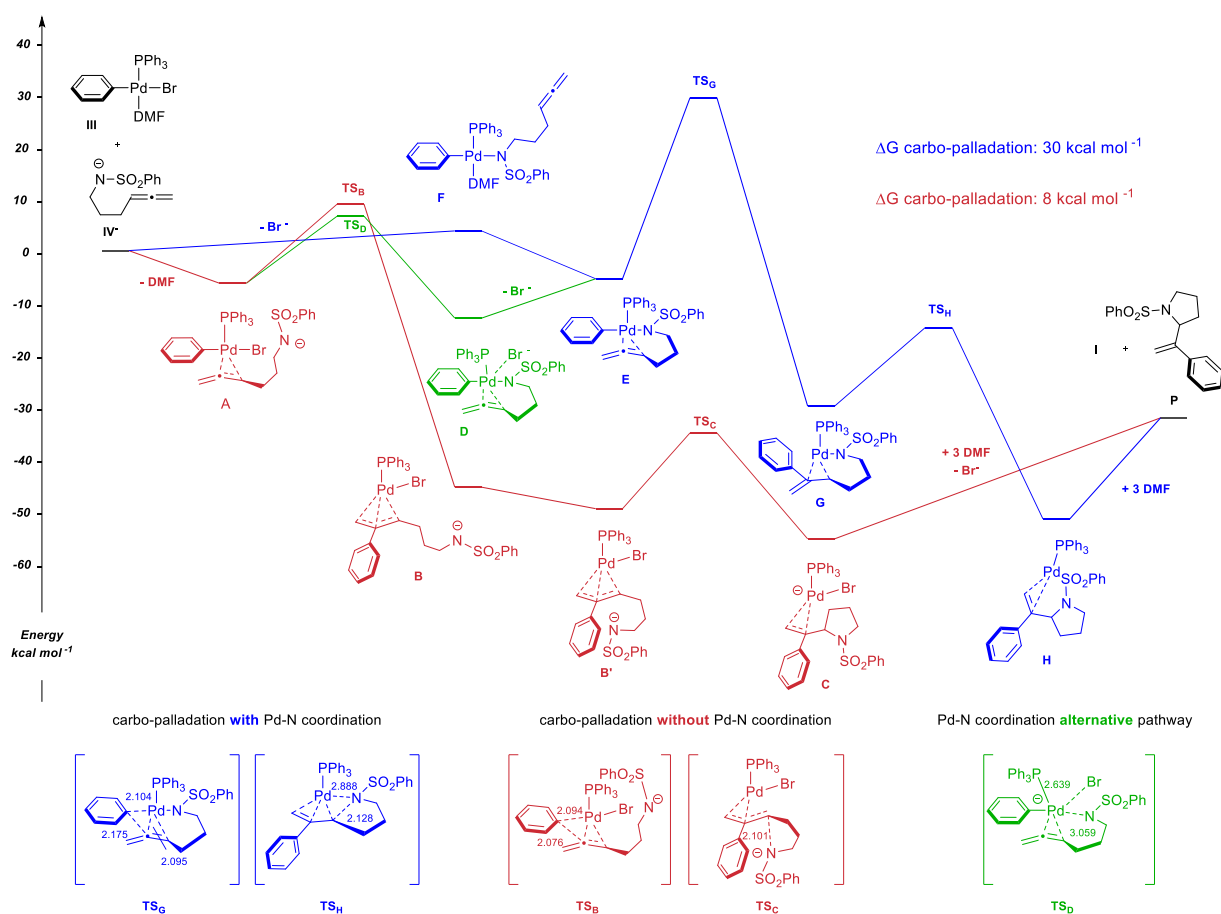

Fig. 5. Energy profiles in kcal mol⁻¹ following the formation of intermediate **III**. The calculation is realised on the deprotonated allene **IV⁻** bearing a phenylsulfonyl moiety instead of a toluenesulfonyl group
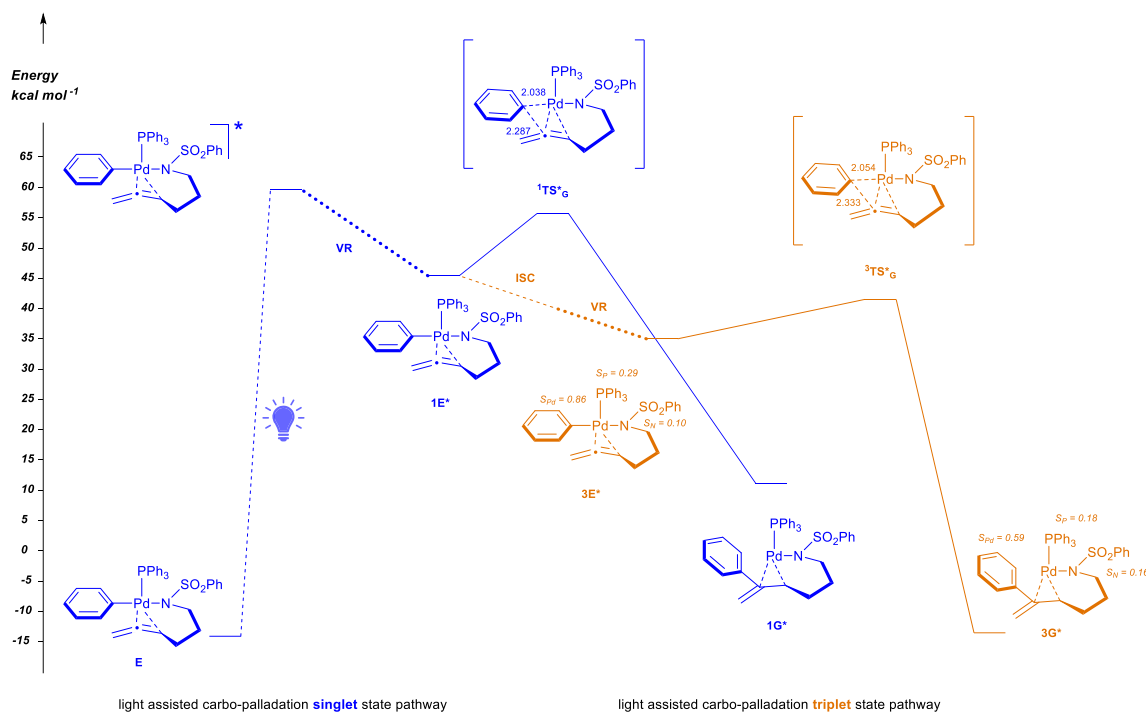
Fig. 6 Energy profiles in kcal mol^{-1} of the photochemical pathways originated from the intermediate **E**. S_X are the atomic spin densities on atom X.

Thanks to an equilibrium among the reactants **III+IV⁻** and the intermediates **A**, **D**, and **E**, we observed that several pathways are accessible. The blue light has the key role of bypassing the thermal **TS$_G$** allowing the carbo-palladation to proceed following an alternative photoinduced route which is not energetically favored in the ground state.

Conclusion

In this paper we presented a synthetic strategy to obtain arylated vinyl pyrrolidines and piperidines starting from *N*-tosylaminoallenes. Key to the process was the usage of the blue light which allowed the efficient exploitation of the simple catalytic system Pd(OAc)$_2$/2PPh$_3$ at room temperature. Electron-donating, electron-withdrawing aryl and heteroaryl bromides were coupled with allenes in a Pd(0) catalysed cross coupling. A subsequent domino cyclisation is triggered by the tosylamino functionality. The mechanistic investigation, both experimental and computational, highlighted three main aspects: no radicals seems to be involved in this mechanism, the light is not needed in the oxidative addition of Pd(0) to the aryl bromide because of the associated low energy barrier. On the contrary, the light plays its main role in the carbo-palladation step, but its influence in making easier the formation of the active Pd(0) species cannot be excluded.

Author Contributions

P. Renzi conceptualization, supervision, investigation, validation and writing; E. Azzi, E. Bessone and S. Parisotto investigation and validation; G. Ghigo formal analysis, methodology and writing of the

computational study; F. Pellegrino UV-vis and CV analysis; A. Deagostino supervision, validation, writing.

Conflicts of interest

There are no conflicts to declare.

Acknowledgements

Notes and references

[]

1. E. Vitaku, D. T. Smith and J. T. Njardarson, *J. Med. Chem.*, 2014, **57**, 10257-10274.
2. R. D. Taylor, M. MacCoss and A. D. G. Lawson, *J. Med. Chem.*, 2014, **57**, 5845-5859.
3. N. Kerru, L. Gummidi, S. Maddila, K. K. Gangu and S. B. Jonnalagadda, *Molecules* 2020, **25**, 1909.
4. P. Bhutani, G. Joshi, N. Raja, N. Bachhav, P. K. Rajanna, H. Bhutani, A. T. Paul and R. Kumar, *J. Med. Chem.*, 2021, **64**, 2339-2381.
5. R. Vardanyan, in *Piperidine-Based Drug Discovery*, ed. R. Vardanyan, Elsevier, 2017, DOI: https://doi.org/10.1016/B978-0-12-805157-3.00002-8, pp. 83-101.
6. R. Vardanyan, in *Piperidine-Based Drug Discovery*, ed. R. Vardanyan, Elsevier, 2017, DOI:

https://doi.org/10.1016/B978-0-12-805157-3.00001-6, pp. 1-82.

7. G. Li Petri, M. V. Raimondi, V. Spanò, R. Holl, P. Barraja and A. Montalbano, *Top. Curr. Chem.*, 2021, **379**, 34.

8. D. O'Hagan, *Nat. Prod. Rep.*, 2000, **17**, 435-446.

9. Y. He, Z. Zheng, J. Yang, X. Zhang and X. Fan, *Org. Chem. Front.*, 2021, DOI: 10.1039/D1QO00171J.

10. C.-V. T. Vo and J. W. Bode, *J. Org. Chem.*, 2014, **79**, 2809-2815.

11. D. Antermite and J. A. Bull, *Synthesis*, 2019, **51**, 3171-3204.

12. A. Hameed, S. Javed, R. Noreen, T. Huma, S. Iqbal, H. Umbreen, T. Gulzar and T. Farooq, *Molecules*, 2017, **22**.

13. A. Deiters and S. F. Martin, *Chem. Rev.*, 2004, **104**, 2199-2238.

14. B. Seifinoferest, A. Tanbakouchian, B. Larijani and M. Mahdavi, *Asian J. Org. Chem.*, 2021, **10**, 1319-1344.

15. I. R. Hazelden, R. C. Carmona, T. Langer, P. G. Pringle and J. F. Bower, *Angew. Chem. Int. Ed.*, 2018, **57**, 5124-5128.

16. N. J. Race, I. R. Hazelden, A. Faulkner and J. F. Bower, *Chem. Sci.*, 2017, **8**, 5248-5260.

17. P. Ruiz-Castillo and S. L. Buchwald, *Chem. Rev.*, 2016, **116**, 12564-12649.

18. S.-M. Wang, H.-X. Song, X.-Y. Wang, N. Liu, H.-L. Qin and C.-P. Zhang, *Chem. Commun.*, 2016, **52**, 11893-11896.

19. C. Colletto, S. Islam, F. Juliá-Hernández and I. Larrosa, *J. Am. Chem. Soc.*, 2016, **138**, 1677-1683.

20. A. Hossian, S. K. Bhunia and R. Jana, *J. Org. Chem.*, 2016, **81**, 2521-2533.

21. M. A. Fredricks, M. Drees and K. Köhler, *ChemCatChem*, 2010, **2**, 1467-1476.

22. D. Kurandina, M. Parasram and V. Gevorgyan, *Angew. Chem. Int. Ed.*, 2017, **56**, 14212-14216.

23. M. Parasram and V. Gevorgyan, *Chem. Soc. Rev.*, 2017, **46**, 6227-6240.

24. P. Chuentragool, D. Kurandina and V. Gevorgyan, *Angew. Chem. Int. Ed.*, 2019, **58**, 11586-11598.

25. K. P. Shing Cheung, S. Sarkar and V. Gevorgyan, *Chem. Rev.*, 2021, DOI: 10.1021/acs.chemrev.1c00403.

26. M. Ratushnyy, M. Parasram, Y. Wang and V. Gevorgyan, *Angew. Chem. Int. Ed.*, 2018, **57**, 2712-2715.

27. D. Kurandina, M. Rivas, M. Radzhabov and V. Gevorgyan, *Org. Lett.*, 2018, **20**, 357-360.

28. M. Parasram, P. Chuentragool, Y. Wang, Y. Shi and V. Gevorgyan, *J. Am. Chem. Soc.*, 2017, **139**, 14857-14860.

29. G.-Z. Wang, R. Shang and Y. Fu, *Org. Lett.*, 2018, **20**, 888-891.

30. G.-Z. Wang, R. Shang, W.-M. Cheng and Y. Fu, *J. Am. Chem. Soc.*, 2017, **139**, 18307-18312.

31. Z. Yang and R. M. Koenigs, *Chem. Eur. J.*, 2021, **27**, 3694-3699.

32. H.-M. Huang, P. Bellotti, P. M. Pflüger, J. L. Schwarz, B. Heidrich and F. Glorius, *J. Am. Chem. Soc.*, 2020, **142**, 10173-10183.

33. M. Koy, F. Sandfort, A. Tlahuext-Aca, L. Quach, C. G. Daniliuc and F. Glorius, *Chem. Eur. J.*, 2018, **24**, 4552-4555.

34. R. Kancherla, K. Muralirajan, B. Maity, C. Zhu, P. E. Krach, L. Cavallo and M. Rueping, *Angew. Chem. Int. Ed.*, 2019, **58**, 3412-3416.

35. W.-J. Zhou, G.-M. Cao, G. Shen, X.-Y. Zhu, Y.-Y. Gui, J.-H. Ye, L. Sun, L.-L. Liao, J. Li and D.-G. Yu, *Angew. Chem. Int. Ed.*, 2017, **56**, 15683-15687.

36. L. Y. Feng, L. Guo, C. Yang, J. Zhou and W. J. Xia, *Org. Lett.*, 2020, **22**, 3964-3968.

37. M. Li, Y.-F. Qiu, C.-T. Wang, X.-S. Li, W.-X. Wei, Y.-Z. Wang, Q.-F. Bao, Y.-N. Ding, W.-Y. Shi and Y.-M. Liang, *Org. Lett.*, 2020, **22**, 6288-6293.

38. A. Deagostino, C. Prandi and P. Venturello, *Org. Lett.*, 2003, **5**, 3815-3817.

39. T. Boi, A. Deagostino, C. Prandi, S. Tabasso, A. Toppino and P. Venturello, *Org. Biomol. Chem.*, 2010, **8**, 2020-2027.

40. S. Parisotto, L. Palagi, C. Prandi and A. Deagostino, *Chem. Eur. J.*, 2018, **24**, 5484-5488.

41. A. Deagostino, C. Prandi, A. Toppino and P. Venturello, *Tetrahedron*, 2008, **64**, 10344-10349.

42. S. Parisotto and A. Deagostino, *Org. Lett.*, 2018, **20**, 6891-6895.

43. C.-H. Yang, M. Han, W. Li, N. Zhu, Z. Sun, J. Wang, Z. Yang and Y.-M. Li, *Org. Lett.*, 2020, **22**, 5090-5093.

44. S. Parisotto and A. Deagostino, *Synthesis*, 2019, **51**, 1892-1912.

45. R. Santhoshkumar and C. H. Cheng, *Asian J. Org. Chem.*, 2018, **7**, 1151-1163.

46. J. T. Ye and S. M. Ma, *Acc. Chem. Res.*, 2014, **47**, 989-1000.

47. J. Le Bras and J. Muzart, *Chem. Soc. Rev.*, 2014, **43**, 3003-3040.

48. M. D. Jovanovic, M. R. Petkovic and V. M. Savic, *Synthesis*, 2021, **53**, 1035-1045.

49. G. L. Li, X. H. Huo, X. Y. Jiang and W. B. Zhang, *Chem. Soc. Rev.*, 2020, **49**, 2060-2118.

50. D. Kurandina, P. Chuentragool and V. Gevorgyan, *Synthesis*, 2019, **51**, 985-1005.

51. O. A. Storozhenko, A. A. Festa, G. I. Detistova, V. B. Rybakov, A. V. Varlamov, E. V. Van der Eycken and L. G. Voskressensky, *J. Org. Chem.*, 2020, **85**, 2250-2259.

52. J. Liu, Y. Wei and M. Shi, *Angew. Chem. Int. Ed.*, 2021, **60**, 12053-12059.

53. R. Tomita, T. Koike and M. Akita, *Chem. Commun.*, 2017, **53**, 4681-4684.

54. J. Singh, A. Sharma and A. Sharma, *Org. Chem. Front.*, 2021, DOI: 10.1039/D1QO00955A.

55. P. Bellotti, M. Koy, C. Gutheil, S. Heuvel and F. Glorius, *Chem. Sci.*, 2021, **12**, 1810-1817.

56. D.-S. Wang, Q.-A. Chen, S.-M. Lu and Y.-G. Zhou, *Chem. Rev.*, 2012, **112**, 2557-2590.

57. A. Bari, A. Iqbal, Z. A. Khan, S. A. Shahzad and M. Yar, *Synth. Commun.*, 2020, **50**, 2572-2589.

58. P. Bellotti, M. Koy, C. Gutheil, S. Heuvel and F. Glorius, *Chem Sci*, 2020, **12**, 1810-1817.

59. M. Koy, P. Bellotti, F. Katzenburg, C. G. Daniliuc and F. Glorius, *Angew. Chem. Int. Ed.*, 2020, **59**, 2375-2379.

60. C. Amatore, A. Jutand and M. A. M'Barki, *Organometallics*, 1992, **11**, 3009-3013.

61. K. Mitsudo, T. Kaide, E. Nakamoto, K. Yoshida and H. Tanaka, *J. Am. Chem. Soc.*, 2007, **129**, 2246-2247.

62. S. Kirchberg, T. Vogler and A. Studer, *Synlett*, 2008, **2008**, 2841-2845.

63. P. Chuentragool, D. Yadagiri, T. Morita, S. Sarkar, M. Parasram, Y. Wang and V. Gevorgyan, *Angew. Chem. Int. Ed.*, 2019, **58**, 1794-1798.

64. N. W. J. Scott, M. J. Ford, N. Jeddi, A. Eyles, L. Simon, A. C. Whitwood, T. Tanner, C. E. Willans and I. J. S. Fairlamb, *J. Am. Chem. Soc.*, 2021, **143**, 9682-9693.

65. N. W. J. Scott, M. J. Ford, C. Schotes, R. R. Parker, A. C. Whitwood and I. J. S. Fairlamb, *Chem. Sci.*, 2019, **10**, 7898-7906.
66. J. N. Harvey, F. Himo, F. Maseras and L. Perrin, *ACS Catal.*, 2019, **9**, 6803-6813.
67. M. García-Melchor, A. A. C. Braga, A. Lledós, G. Ujaque and F. Maseras, *Acc. Chem. Res.*, 2013, **46**, 2626-2634.
68. M. Besora and F. Maseras, *Dalton Trans.*, 2019, **48**, 16242-16248.